AGU ADVANCING EARTH AND SPACE SCIENCE

Geophysical Research Letters®

RESEARCH LETTER
10.1029/2021GL096957

Key Points:

- A framework to characterize the dynamic connectivity emerging from the transport of fluxes on river networks is introduced
- The abundance of side-branching junctions (accelerates) decelerates the timing to full connectivity under (low) peak flow conditions
- Humid basins exhibit topologies which are prone to slow-down the convergence of fluxes

Supporting Information:

Supporting Information may be found in the online version of this article.

Correspondence to:

A. Singh,
Arvind.Singh@ucf.edu

Citation:

Roy, J., Tejedor, A., & Singh, A. (2022). Dynamic clusters to infer topologic controls on environmental transport of river networks. *Geophysical Research Letters*, *49*, e2021GL096957. https://doi.org/10.1029/2021GL096957

Received 8 NOV 2021
Accepted 25 FEB 2022

Dynamic Clusters to Infer Topologic Controls on Environmental Transport of River Networks

Juthika Roy[1], Alejandro Tejedor[2,3], and Arvind Singh[1]

[1]Department of Civil, Environmental and Construction Engineering, University of Central Florida, Orlando, FL, USA, [2]Department of Science and Engineering, Sorbonne University Abu Dhabi, Abu Dhabi, UAE, [3]Department of Civil and Environmental Engineering, University of California Irvine, Irvine, CA, USA

Abstract The knowledge of structural controls of river networks (RNs) on transport dynamics is important for modeling and predicting environmental fluxes. To investigate impacts of RN's topology on transport processes, we introduce a systematic framework based on the concept of dynamic clusters, where the connectivity of subcatchments is assessed according to two complementary criteria: minimum- and maximum-flow connectivity. Our analysis from simple synthetic RNs and several natural river basins across the United States reveals the key topological features underlying the efficiency of flux transport and aggregation. Namely, the timing of basin-scale connectivity at low-flow conditions is controlled by the abundance of topologically asymmetric junctions (side-branching), which at the same time, result in a slow-down of the flux convergence at the outlet (maximum-flow). Our results, when compared with observed topological trends in RNs as a function of climate, indicate that humid basins exhibit topologies which are "naturally engineered" to slow-down fluxes.

Plain Language Summary In this study, we develop a systematic framework that characterizes the evolution of flux movement on a river network and quantifies the control exerted by the channel structure and connectivity on the environmental transport processes. Using both synthetically generated river networks as well as several natural river basins with minimum human impact across the United States, we explore the relative role of branching channels versus side-tributaries. Our results show that the abundance of side-tributaries have opposite implications on the timing at which the basin achieves full connectivity: faster convergence at minimum-flow conditions, while slower aggregation of fluxes at the outlet (peak flow) of the river network. Our study indicates that the connectivity of river networks, and therefore their efficiency in aggregating fluxes, differ in humid and arid environments.

1. Introduction

Drainage basins are the regions where precipitated rainfall advances downhill as runoff and accumulates to form river channels. The hierarchically connected river network (RN) drains the basin and serves as a primary passage for carrying spatially and temporally varying environmental fluxes such as water, sediment, and nutrients (Benda et al., 2004; Cushman & McGarigal, 2002; Hansen & Singh., 2018; Kiffney et al., 2006). Thus, the branching structure of a river plays a fundamental role in biodiversity, exchanging nutrients between ecosystems, maintaining migration routes for aquatic lives, among others (Convertino et al., 2007; Perron et al., 2012; Rice et al., 2006; Rigon et al., 1996; Rodriguez-Iturbe et al., 2009; Stewart-Koster et al., 2007). However, RNs are facing unprecedented disturbances at global scale under changing human activities (e.g., intensification of land-use and forest-fires) and climate (e.g., change of precipitation patterns), leading to potential changes in the river structure and its response in its capacity of transporting fluxes (Prancevic & Kirchner, 2019; Ward et al., 2020). In addition, it has been recognized that the complex runoff response of a basin, which is driven by its physical attributes (e.g., drainage-network patterns, topography, basin shape, etc.), hinders our ability to draw causal relations between the properties of its RN, and their impact on the transported fluxes (Czuba & Foufoula-Georgiou, 2015; Zaliapin et al., 2010).

A significant research has been conducted since past several decades on the branching structure of RNs to address their topological and geomorphological connections with hydrological responses. Major breakthroughs include the development of unit hydrograph by the formulation of width function (Gupta et al., 1986; Kirkby, 1976; Marani et al., 1991; Mesa & Mifflin, 1986; Troutman & Karlinger, 1985), the advancement of the instantaneous and the geomorphological instantaneous unit hydrographs (Gupta et al., 1980; Rodriguez-Iturbe & Valdes, 1979),

for example. These advances enable us to analyze the spatio-temporal performance of the network under the runoff operation. Thus, the evolution of methodical frameworks based on the concept of system response toward the transport processes on the RNs stays in the place of substantial interest in hydrology and earth and environmental sciences (Collischonn et al., 2017; Garbin et al., 2019; Li & Sivapalan, 2011).

The structural connectivity of a RN, that is, how the different channels connect, can be fully represented as a topological object, a graph (also referred to as network) (Carstens, 2017; Scheidegger, 1967). Particularly, the connectivity of RN tributaries corresponds universally to tree networks, whose prevalence has been argued in terms of optimality (Rodriguez-Iturbe & Rinaldo, 2001). The topological properties of RNs have been studied in detail (Horton, 1945; Shreve, 1966; Strahler, 1957; Tokunaga, 1978), pointing out the importance of branching (junctions of same order channels) versus side-branching (junctions of different order channels) structures in RN characterization. Lately, some studies analyzed the contribution of branching versus side-branching to examine the impact of different climates on RNs (Abed-Elemdoust et al., 2016; Ranjbar et al., 2018; Zanardo et al., 2013). These works mainly explored the structural connectivity of RNs with varying precipitation patterns.

The main goal of this study is to understand and quantify the role of side-branching of a RN in transporting fluxes. To achieve this, we introduce the concept of dynamic clusters to characterize the connectivity of channels emerging from flux propagation on the RN. The proposed dynamic connectivity framework can quantify time-dependent cluster formation based on the concept of structural extent (connectivity at minimum flow) and aggregated flux connectivity (connectivity at maximum flow). This framework is applied to both synthetic and natural RNs to systematically explore and understand the roles of different channel connectivity and arrangements in transporting fluxes through RNs.

2. Dynamic Connectivity and Clustering

A cluster commonly denotes a set of connected elements, which are disconnected from other elements in the system. For a network, a cluster corresponds to a set of connected nodes (or equivalently links) such that it is possible to find a path between any pair of nodes in that set; the nodes belonging to a cluster are disconnected from the rest of the nodes in the network.

Here, we conceptualize the RN connectivity as a binary tree network, wherein nodes represent junctions and links represent streams (also referred to as channels). The term binary refers to the fact that each junction, here denoted as an internal node, is the result of merging two upstream channels. Beyond characterizing the connectivity of the static network of RN (e.g., obtained from the digital elevation model (DEM) using a flow-routing algorithm) via cluster analysis, it is important to explore the dynamic connectivity emerging on that static network as fluxes propagate. The dynamic connectivity, although driven by the underlying static structure (structural connectivity), depends also on the nature of the transport process considered (e.g., fluxes transported from channel heads to outlet) (Larsen et al., 2012; Wohl et al., 2019). Furthermore, dynamic connectivity depends on the property that needs to be satisfied to assume that two streams are dynamically connected (e.g., links become connected as a flux progresses through them), and therefore they are in the same cluster. In the following subsections, we introduce first the flux propagation to define the dynamic connectivity, and then two different criteria to define clusters, namely, dynamic clusters based on the network's structural extent and dynamic clusters based on time of concentration (aggregated flux connectivity).

2.1. Flux Propagation on a Network

Following the approach introduced by Zaliapin et al. (2010), we define an idealized transport process, where tracers are simultaneously and continuously introduced at all source nodes (N_s) in the RN. The tracer fluxes propagate and aggregate as they travel downstream in the network. By examining the patterns that emerge from transport of fluxes in the networks with different topologies, we can potentially draw relationships between network topologies and the nature of flux propagation patterns emerging in the system. The emergent connectivity is interrogated by analyzing the temporal evolution of clusters (as defined in the next two subsections) in the network as the flux propagates from the source nodes towards the basin outlet. These clusters are called dynamic clusters for two main reasons: (a) they are emerging from a dynamic process—propagation of fluxes; and (b) the number of clusters, and their size evolve over time as transport proceeds.

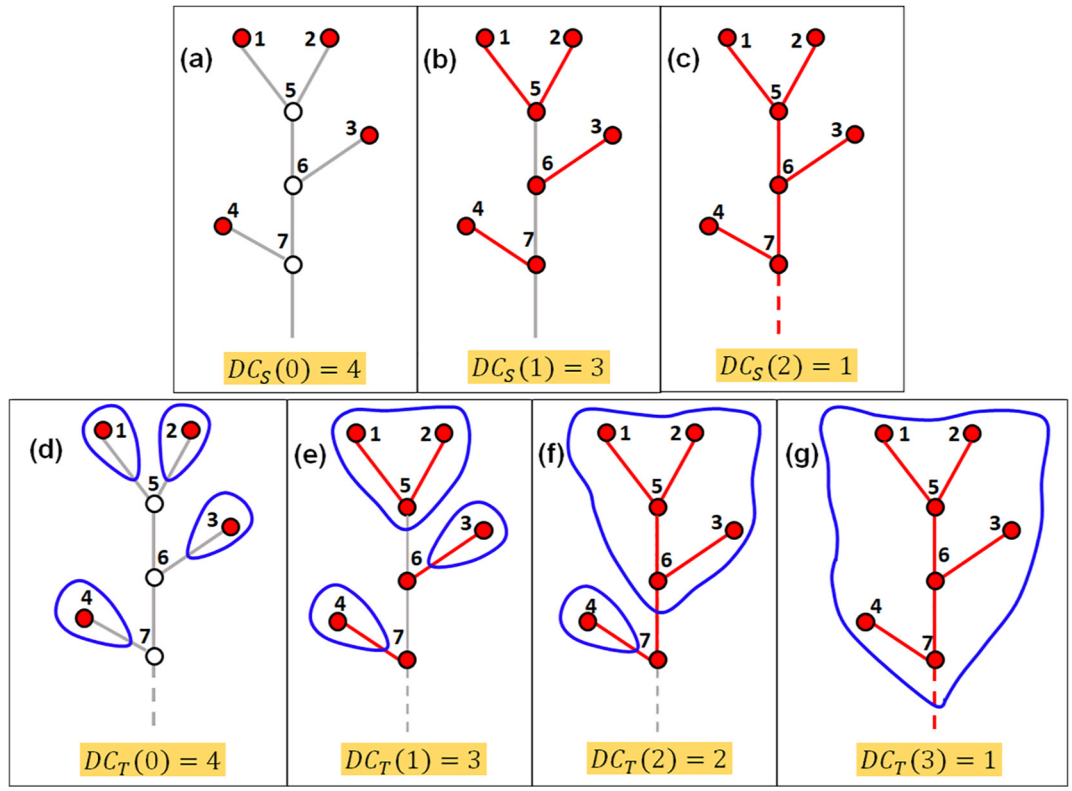

Figure 1. Evolution of dynamic clusters on a river network based on (a–c) structural extent, and (d–g) aggregated flux connectivity (TOC). The blue envelops in d, e, f, and g indicate clusters.

It is important to note that our flux propagation framework is general, and the transport process can be implemented with different levels of detail. For instance, the morphologic properties of each stream in the river basin can be incorporated to acknowledge more realistic transport dynamics and travel times (Czuba & Foufoula-Georgiou, 2014, 2015). This could be particularly relevant to model sediment fluxes allowing spatially distributed sources with varying production rates in the network. However, in our study we aim to identify the key topological properties of RNs, which control flux propagation processes. For this reason, and to enhance the interpretability of our results, we simplify the problem under study by assuming that all streams in the network have constant length, and the tracer fluxes propagate downstream at a constant velocity. Thus, differences in the emerging aggregation properties can be solely attributed to differences in the topological properties of the RNs.

2.2. Dynamic Clusters Based on Structural Extent (DC_S)

At the beginning of the flux propagation process, each source node is considered as an independent cluster, thus the system is defined by N_s clusters, each of them of size 1 (here, we define the size of a cluster as the number of source nodes in that cluster). As tracer fluxes propagate downstream of each source node, internal nodes are reached by tracer fluxes. Given the tree structure of RNs, every internal node corresponds to a junction, where tracer fluxes originating from different source nodes will combine at different stages of the flux propagation process. We define the merging of two clusters X and Y to form a cluster Z, when tracer fluxes coming from one of the sources contained in cluster X reach a junction where tracer fluxes originated within cluster Y are propagating. The size of the newly formed cluster Z is simply defined as the sum of the sizes of clusters X and Y (see Figures 1a–1c for illustration). Formally, obtaining this cluster type corresponds to the so-called hierarchical nearest neighbor clustering (HNNC). The HNNC method (for further details, see Figure S1 and Section S2 in Supporting Information S1) is based on the distance matrix, which is a square symmetric matrix containing pairwise distance between every cluster which can be expressed as,

$$d(X, Y) = min\left[d\left(X_a, Y_a\right)\right], \tag{1}$$

where X and Y are two clusters, each containing a different subset of source nodes. $X = \{X_a\}_{a=1.....N_X}$ and $Y = \{Y_a\}_{a=1.....N_Y}$. N_X and N_Y correspond to the number of source nodes in cluster X and Y, respectively. The distance $d(X, Y)$ is defined as the minimum pairwise distance between the sources of the two clusters. Thus, this formalism allows to identify the clusters merging at every time step, namely, the clusters exhibiting the smallest distance. Note that after each cluster merges, the distance matrix is updated. Based on this algorithm, the number of clusters is computed at every proceeding time t (recall, $DC_S(t = 0) = N_s$). The subscript S in $DC_S(t)$ emphasizes that clusters correspond to the dynamic response of the system in terms of the structural extent of the RN which is concurrently activated as fluxes propagate. Note that this definition of cluster is particularly relevant in terms of environmental fluxes, since given a cluster, all channels within that cluster are guaranteed to transport tracer fluxes from at least one of the source nodes. Thus, a cluster can be interpreted as a joint spatial extent of the channel network where a minimum flow has been achieved.

2.3. Dynamic Clusters Based on Time of Concentration (DC_T)

The dynamic connectivity based on structural extent (DC_S) requires that the spatial connection of the streams is achieved via flux propagation; however, it does not require that all different tracer fluxes from all source nodes in a given cluster are aggregated (mixed) and contribute to most downstream node in that cluster. In other words, from a perspective of structural connectivity, the definition of a cluster does not imply that the peak discharge is achieved in the most downstream stream in that cluster. For quantifying the connectivity induced by the aggregation of fluxes, we utilize the same flux propagation process, wherein tracer fluxes are introduced continuously in the network via all the source nodes, leading to an initial configuration where each source node is considered as an independent cluster. However, the rule for two clusters to merge is that the two clusters share a common downstream node which has achieved maximum flow (see Figures 1d–1g for illustration). Alternatively defined, the upstream network of a given node consists of a single cluster if the time of concentration (TOC—time at which the maximum possible discharge is observed at that node) of such node is achieved; the size of such a cluster is equal to the total number of source nodes in that cluster (see also Figure S2 and Section S3 in Supporting Information S1). From this definition, it is evident that the entire RN will attain full connectivity, that is, the whole RN is characterized by a single cluster, at a time equal or larger than the TOC of the basin, which corresponds to the time taken by the tracer injected at the most distant source node to reach the basin outlet. Thus, the dynamic connectivity of the RN is characterized by the temporal evolution of the number of clusters $DC_T(t)$ emerging at different stages of the flux propagation process. The subscript T emphasizes that clusters correspond to the dynamic response of the system in terms of the aggregation of fluxes or TOC of the most downstream node in the cluster.

3. Dynamic Connectivity in Synthetic River Networks

In order to identify the key topological features of RNs that control the evolution of the dynamic connectivity (both as described by $DC_S(t)$ and $DC_T(t)$), we utilize five simple synthetic networks (SNs), each of them consisting of 31 nodes: 16 source nodes and 15 internal nodes (see Figures 2a–2e). Despite the simplicity of these networks, they allow us to explore a wide range of topologies in terms of side-branching structures, including the end-members with no side-branches, SN_{br} (i.e., all junctions are formed by two upstream branches of the same Horton-Strahler order; Horton, 1945; Strahler, 1957) (Figure 2a) and with the maximum number of side-branches, SN_{sbr} (i.e., there is only one junction wherein two streams of the same order meet and all the other junctions correspond to side-branches) (Figure 2e).

3.1. Dynamic Connectivity: Structural Extent (DC_S)

For each of the SNs, we computed the number of dynamic clusters, $DC_S(t)$ as a function of time steps t (see Figure 2f). We observe that the proportion of side-branching in the network constitutes a first-order control on the number of time steps needed to achieve full connectivity ($DC_S = 1$), where, generally, the larger the proportion of side-branching, the fewer the number of steps to achieve complete structural connectivity (see Table S1 in Supporting Information S1).

To better compare DC_S trends for networks that require different time to achieve full connectivity, we introduce the normalized versions of DC_S and t, namely DC_S^* and t^*, such that they vary in the interval [0,1] (i.e., at $t = 0$:

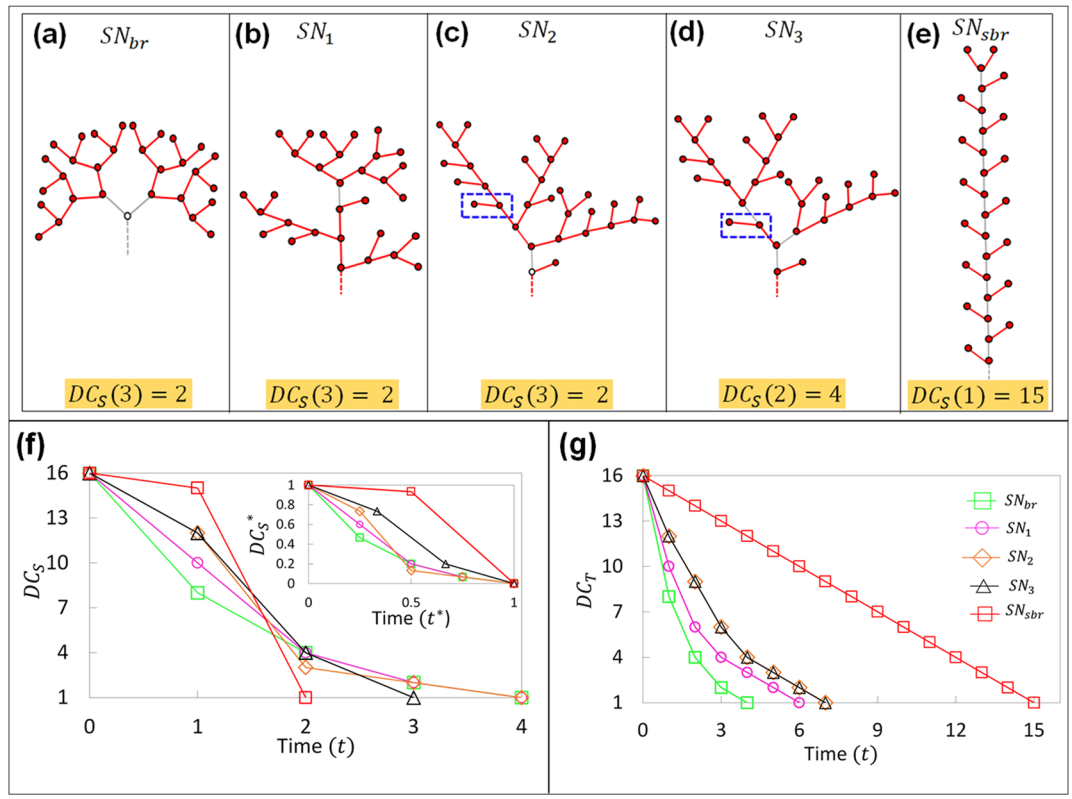

Figure 2. (a)–(e) Schematics of five different SNs with 16 source nodes. (a) SN_{br} (Horton-Strahler order, HS = 5), (b) SN_1 (HS = 4), (c) SN_2 (HS = 4), (d) SN_3 (HS = 4), and (e) SN_{sbr} (HS = 2). (f) Cluster evolution of the SNs based on structural extent, DC_S and normalized DC_s^* (inset). (g) Cluster evolution of the SNs based on aggregated flux connectivity (TOC), DC_T.

$t^* = 0$ and $DC_S{}^* = 1$; and at the time when the RN achieves full connectivity: $t^* = 1$ and $DC_S{}^* = 0$). The evolution of the connectivity for the two end-member topologies in terms of the $DC_S{}^*$ versus t^* reveals a change in the overall concavity of the curves: we observe a concave-up shape for $DC_S{}^*$ in the case of purely branching structure (see inset in Figure 2f), while the trend becomes concave-down when the end-member with the maximum number of side-branches is examined (see Section 2 in Supporting Information S1 for analytical formulation of $DC_S{}^*$ vs. t^*). For any given network, the temporal evolution of $DC_S{}^*$ is thus constrained between the trend corresponding to the two endmembers. Hence, as the network exhibits a higher fraction of internal nodes corresponding to a side-branching junction, the evolution of $DC_S{}^*$ diverges from the concave-up shape. This general trend is verified from our analysis of the five SNs shown in the inset of Figure 2f.

In order to explore the effect of the spatial arrangement of side-branches in the dynamic connectivity, we analyze two SNs consisting of the same side-branching ratio, where the spatial location of two side-branches are swapped (Figures 2c and 2d show the same SN structure differing only in the spatial location of the side-branches enclosed in the blue dashed box). We observe that the number of steps to achieve full connectivity differs for those two networks indicating the relevant role of the spatial location of side-branches in the evolution of $DC_S(t)$. To quantify the effect of side-branching proportion and their spatial location, we define d_{iS^*} as the distance from internal node i to its closest upstream source S^*. Thus, internal node i, requires d_{iS^*} time steps (note that for a varying velocity, d_{iS^*} can be transformed to its corresponding time) to be reached by a tracer flux, and become a part of a cluster. Consequently, a node k characterized by the largest distance to the source, d_{kS^*}, controls the number of steps to achieve full structural connectivity of a RN. With this understanding, one can interpret our previous observations and infer the following key topological features controlling structural connectivity: (a) increasing side-branching accelerates the rate to achieve structural connectivity—the presence of side-branches reduces the distance of internal nodes to sources as compared with branching structures, therefore reducing the values of d_{iS^*}. (b) The large difference in the order of side-branching with respect to the order of the main branch leads to faster convergence to structural connectivity—the spatial arrangement of low-order side-branches tend to reduce the

d_{iS^*} of the internal nodes, accelerating the merging of dynamic clusters, and achieving a larger coverage of the structural extent of the network in fewer steps.

3.2. Dynamic Connectivity: Time of Concentration (DC_T)

We now utilize the same SNs (see Figures 2a–2e) to identify the topological properties of RN that control the aggregation of fluxes as quantified via $DC_T(t)$. We observe that the proportion of side-branching in the network plays a fundamental role in the evolution of $DC_T(t)$, and particularly in the number of time steps t, needed to achieve full connectivity ($DC_T = 1$), where, generally, the larger the proportion of side-branching, the larger the number of steps to attain full connectivity (Figure 2g). Thus, when we compare the evolution of the connectivity for the two end-member topologies: (a) SN_{sbr} (Figure 2e) exhibits a linear decrease of DC_T as a function of time (Figure 2g). The slope of such a linear relationship is one (i.e., there is merging of only two clusters per unit of time), establishing the slowest convergence possible and the largest TOC for a given number of nodes in the network. (b) Given that we are only considering binary trees, SN_{br} (Figure 2a) shows the fastest possible decline of $DC_T(t)$ (Figure 2g); specifically, it decreases as $\frac{N_s}{2}$.

For other SN topologies, $DC_T(t)$ curves do not change in overall concavity (no transition from concavity to convexity as observed in our analysis of $DC_S(t)$). To quantify the rate at which the RN is achieving dynamic connectivity, we define the ICR (integral connectivity rate) as the area under the $DC_T(t)$ curve. Note that the larger the ICR is, the slower is the convergence of the RN to obtain aggregated flux connectivity (see ICR values for SNs in Table S1 in Supporting Information S1). The two end-member topologies establish the upper and lower bound for the evolution of the dynamic connectivity based on flux aggregation in terms of TOC (and thus ICR). The other SNs used in the analysis (Figures 2b–2d) lay in between, presenting a general decreasing trend of their dynamic connectivity (Figure 2g) with respect to the percentage of the side-branching.

It is important to highlight that the evolution of the dynamic connectivity based on flux aggregation is also sensitive to the spatial arrangement of side-branches. However, not all the alternative topologies consisting of the same side-branching structures (different spatial configurations, e.g., Figures 2c and 2d) exhibit different evolution of $DC_T(t)$. The key point to consider evaluating if the different spatial arrangements lead to a different dynamic response is whether that spatial rearrangement modifies the TOC for any node in the network. For instance, the topologies shown in Figures 2c and 2d have the same side-branches, where two of them are spatially re-arranged. However, this rearrangement does not imply any change in TOC of any node in the RN, and therefore the whole $DC_T(t)$ remains same. On the other hand, changes that imply modification of the local TOC of any node in the RN or the TOC of the basin reflect in the temporal evolution of DC_T (see Figure S3 in Supporting Information S1). The implications of these findings for general RNs are apparent: for asymmetric junctions (here defined as junctions where two upstream subcatchments of very different sizes and TOCs merge) the DC_T is controlled by the largest upstream subcatchment. These results indicate that the presence of side-branches with larger differences in Horton-Strahler order (statistically asymmetric junctions) play the most relevant role in decelerating the convergence rate to achieve full dynamic connectivity of a RN in terms of flux aggregation.

4. Dynamic Connectivity in Natural River Networks

In this section, we explore the dynamic connectivity of natural river networks (NRNs) emerging from the described flux propagation process. We selected 50 natural river basins, with minimum human impact, located in different geographic regions across the United States (see Figure S4 in Supporting Information S1). These basins correspond to drainage area from 0.15 to 4.37 km^2 and mean-annual precipitation from 80.8 to 3838 mm. The channel networks for these basins were extracted from 1 m resolution DEMs. In this study, we use slope-area method (McNamara et al., 2006; Montgomery & Foufoula-Georgiou, 1993; Tarboton et al., 1992) to ensure the extracted networks are within the alluvial regime. The threshold for the channel network extraction for each RN was selected in such a way that each extracted network consisted of exactly 64 source nodes. Similar to SNs, we interrogate the NRNs' dynamic connectivity by examining the number of clusters, both DC_S and DC_T, as a function of the flux propagation stage (time). For comparison, we include in our analysis the two end-members SNs (one with complete branching SN_{br} and another with maximum side-branching SN_{sbr}) with 64 source nodes.

Figure 3a shows the DC_S evolution curves for the NRNs and reveals the emergence of two subsets of NRNs: (a) set R1 consists of 18 NRNs, which are characterized by a slower decline of the number of clusters over time and

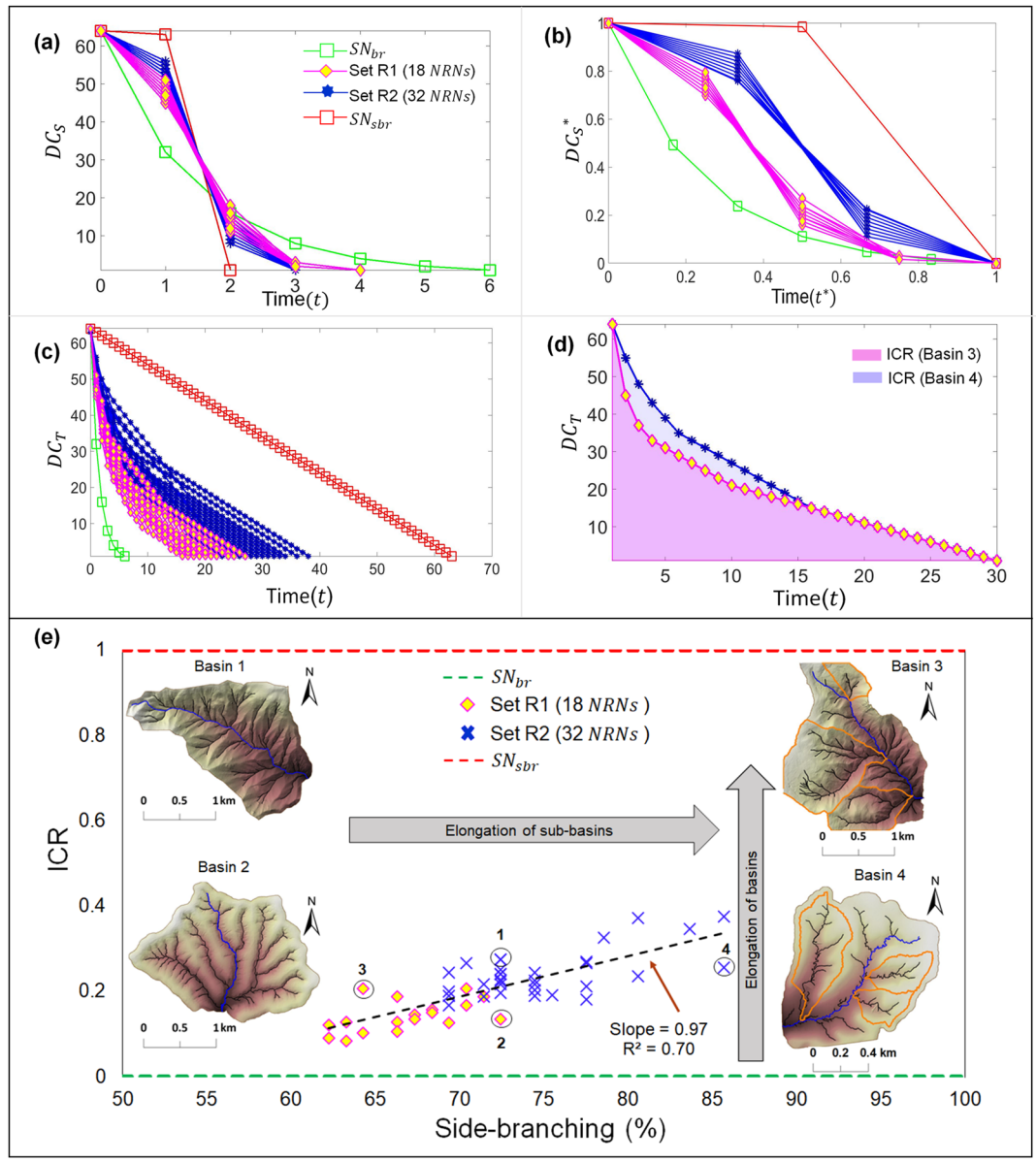

Figure 3. Cluster evolution of the NRNs based on the (a) structural extent, DC_S (b) normalized structural extent, DC_s^*, and (c) aggregated flux connectivity, DC_T. (d) Cluster evolution (DC_T) of the networks of Basins 3 and 4 with similar TOC (i.e., time to reach complete flux connectivity) but different ICR (integral connectivity rate). (e) Relationship between ICR and side-branching for NRNs. Note that ICR here is normalized such that ICR = 0 for the SN_{br} and ICR = 1 for SN_{sbr}.

larger number of steps to achieve full structural connectivity; (b) set R2 consists of 32 NRNs, which require a shorter time to achieve full connectivity. When $DC_S(t)$ is normalized between 0 and 1, the separation of the two subset R1 and R2 is even more apparent, and, as expected, the DC_S curves for all NRNs fall within the envelope delineated by DC_S^* computed for SN_{br} and SN_{sbr} (see Figure 3b).

From our study using SNs, we hypothesized that the decline of DC_S is mostly controlled by the proportion of side-branching in the RN. When we compute this proportion for the two subset of NRNs, R1 and R2, obtained from the analysis of their dynamic connectivity, we indeed find a statistically significant difference (tested using Mann-Whitney-Wilcoxon test for significance within 95% confidence interval (Mann & Whitney, 1947; Wilcoxon, 1945)) in their proportion of side-branching, where basins in the R2 group exhibit higher side-branching proportion (approximately 75%) as compared to R1 (approximately 67%). These results indicate that the

proportion of side-branching versus branching junctions acts as a first-order control on the dynamic connectivity based on the structural extent of RNs.

NRNs are also analyzed for dynamic connectivity based on TOC. Figure 3c shows DC_T as a function of time for NRNs. Similar patterns as discussed for SNs are observed, that is, networks with higher side-branching exhibit slower convergence of fluxes. Although, in general, the DC_T curves of NRNs (see Figure 3d for illustration) show difference between sets R1 and R2, the separation of the two sets is not as distinct as seen from the DC_S curves. For this reason, we compute the ICR for each NRNs and explore its dependence as a function of side-branching ratio (Figure 3e). The following observations can be made from Figure 3e: (a) a positive trend between ICR and side-branching ratio can be seen suggesting that networks with higher side-branching ratio take longer to achieve complete flux connectivity; (b) the variability observed with respect to the linear trend can be interpreted according to the understanding gained from the analysis of SNs. Namely, the same side-branching ratio can generate different DC_T (ICR), due to the spatial location of the side-branches, and more specifically, due to the junction asymmetry. Thus, highly asymmetric junctions (implying more elongated basins and sub-basins) are characterized by a larger ICR (even for the same side-branching ratio). In Figure 3e, two basins characterized with the same side-branching ratio, Basin 1 and Basin 2 (shown as insets), confirm that the more elongated basin exhibits a larger ICR and thus TOC. To quantify drainage basin shape, Schumm (1956) suggested elongation ratio, R_e, expressed as:

$$R_e = \frac{1}{L_b}\sqrt{(4/\pi)A_W} \tag{2}$$

where, L_b is the maximum basin length or main channel length and A_w is the drainage area (Schumm, 1956). Based on R_e, basins can be classified as more elongated ($R_e < 0.5$), elongated ($R_e \sim 0.5$–0.7), and less elongated ($R_e \sim 0.7$–0.8) (Schumm, 1956). Following Equation 2, R_e is 0.56 for the Basin 1 and 0.77 for the Basin 2. Therefore, Basin 1 is more elongated than Basin 2, which further supports our observations and arguments given above about the effect of basin shape on ICR (or TOC) (see also Figure S5 in Supporting Information S1).

It is worth noting that the variability shown in Figure 3e allows the existence of basins with very different side-branching ratios, but similar ICR (e.g., Basins 3 and 4 exhibiting same TOC—see Figure 3d and insets of Figure 3e). We argue that this horizontal variability is controlled by the geometry of the sub-basins, particularly, sub-basin elongation. Thus, when R_e is computed for some representative sub-basins (selected based on their main-stream length and the number of sources) of Basins 3 and 4 (marked with orange boundary-line in the insets of Figure 3e), it is observed that sub-basins ($R_e \sim 0.50$) from Basin 4 are more elongated than those from Basin 3 ($R_e \sim 0.78$).

5. Summary and Concluding Remarks

RNs are geomorphic features that support landscapes for transporting and distributing environmental fluxes such as water, sediment, and nutrients heterogeneously throughout the network and provide hierarchical habitats to the freshwater species as well as act as pathways for pathogens of life-threatening water-borne diseases. The spatial dynamics and the induced heterogeneity in spreading of the biological and ecological communities are affected by the network structure (Muneepeerakul et al., 2008; Rodriguez-Iturbe et al., 2009).

To understand and quantify the effect of the RN structure on the organization and accumulation process of environmental fluxes, we investigate the topological controls of RNs subjected to transport activity using synthetic and natural river networks. We developed a dynamic connectivity framework that characterizes the dynamic patterns emerging from transport processes on RNs. Within the framework, we evaluate the dynamic connectivity of RNs by examining the emerging clusters based on structural extent (DC_S) and time of concentration (DC_T). DC_S provides information about the dynamic connectivity at minimum flow, whereas, DC_T provides information about the emerging connectivity at maximum flow conditions. Our results suggest that the fraction of side-branching versus branching junctions acts as a first-order control on the dynamic connectivity based on the structural extent of river networks. In comparison to structural connectivity, the impact of side-branching on flux connectivity is entirely different. The results indicate that networks with higher side-branching ratio take longer to achieve complete flux aggregation connectivity.

Previous research has shown a dependence of the structure of RNs on geologic, climatic, and human activities (Durighetto & Botter, 2021; Hooshyar et al., 2019; Jensen et al., 2019; Sassolas-Serrayet et al., 2018; Singh et al., 2015; Tejedor et al., 2017; Willett et al., 2014). Particularly, the dependence of side-branching on climatic variables has been argued (Ranjbar et al., 2018; Zanardo et al., 2013), wherein humid landscapes are reported to exhibit a larger ratio of side-branching to branching structures. Our study of the dynamic connectivity of NRNs draws further implications in terms of the dynamic response of RNs in different climatic regions: humid basins are drained by river networks with higher side-branching ratios, which establish a *topological brake* slowing down the convergence of fluxes, and therefore, are able to hold fluxes for longer time, delaying the accumulation of fluxes, while networks in arid basins accelerate this process. On the other hand, from the structural connectivity point of view, RNs in humid environments facilitate the emergence of larger connected spatial extents faster than for arid environments. Our results are of particular relevance given that RNs are facing unprecedented changes in their structure and functions due to changing climatic and human activities. For instance, these results potentially indicate that under a climate-change scenario, wherein extreme events are expected to intensify in the frequency and magnitude (Feng et al., 2013; Ingram, 2016; Papalexiou & Montanari, 2019), the risk of flooding would be exacerbated in arid environments, whose network topologies are not naturally evolved to sustain the fluxes for relatively longer times, and therefore attaining faster peak-flow magnitudes.

The dynamic connectivity framework presented here can be generalized to interrogate the impact of other relevant parameters (e.g., channel geometry, varying flow velocities, and heterogeneous precipitation patterns) on flux transport and aggregation, allowing us to explore the compound effects of those parameters together with topology in the phenomena and scenarios discussed above. A particularly pertinent application of this framework could arise by incorporating the ephemerality (i.e., persistence of streamflow) of the streams to understand the river response in the face of the spatial heterogeneity introduced by the local ecohydrology of the basin (Botter et al., 2021). This phenomenon can induce a significant impact on the hierarchical aggregation of streamflow, which can be further interpreted in conjunction with the topology via the proposed framework.

Data Availability Statement

The data of the DEMs for the natural catchments can be downloaded from https://doi.org/10.5281/zenodo.5637518.

Acknowledgments
Arvind Singh acknowledges partial support from the National Science Foundation (NSF) grant EAR-1854452. The authors thank the Editor, Associate Editor, G. Botter, and an anonymous reviewer, whose suggestions and constructive comments substantially improved our presentation and refined our interpretations.

References

Abed-Elmdoust, A., Miri, M. A., & Singh, A. (2016). Reorganization of river networks under changing spatiotemporal precipitation patterns: An optimal channel network approach. *Water Resources Research*, *52*(11), 8845–8860. https://doi.org/10.1002/2015WR018391

Benda, L. E. E., Poff, N. L., Miller, D., Dunne, T., Reeves, G., Pess, G., & Pollock, M. (2004). The network dynamics hypothesis: How channel networks structure riverine habitats. *BioScience*, *54*(5), 413–427. https://doi.org/10.1641/0006-3568%282004%29054%5B0413:tndhhc%5D2.0.co;2

Botter, G., Vingiani, F., Senatore, A., Jensen, C., Weiler, M., McGuire, K., et al. (2021). Hierarchical climate-driven dynamics of the active channel length in temporary streams. *Scientific Reports*, *11*(1), 1–12. https://doi.org/10.1038/s41598-021-00922-2

Carstens, C. J. (2017). Topology of complex networks: Models and analysis. *Bulletin of the Australian Mathematical Society*, *95*(2), 347–349. https://doi.org/10.1017/S0004972716001003

Collischonn, W., Fleischmann, A., Paiva, R. C., & Mejia, A. (2017). Hydraulic causes for basin hydrograph skewness. *Water Resources Research*, *53*(12), 10603–10618. https://doi.org/10.1002/2017WR021543

Convertino, M., Rigon, R., Maritan, A., Rodriguez-Iturbe, I., & Rinaldo, A. (2007). Probabilistic structure of the distance between tributaries of given size in river networks. *Water Resources Research*, *43*(11). https://doi.org/10.1029/2007WR006176

Cushman, S. A., & McGarigal, K. (2002). Hierarchical, multi-scale decomposition of species-environment relationships. *Landscape Ecology*, *17*(7), 637–646. https://doi.org/10.1023/A:1021571603605

Czuba, J. A., & Foufoula-Georgiou, E. (2014). A network-based framework for identifying potential synchronizations and amplifications of sediment delivery in river basins. *Water Resources Research*, *50*(5), 3826–3851. https://doi.org/10.1002/2013WR014227

Czuba, J. A., & Foufoula-Georgiou, E. (2015). Dynamic connectivity in a fluvial network for identifying hotspots of geomorphic change. *Water Resources Research*, *51*(3), 1401–1421. https://doi.org/10.1002/2014WR016139

Durighetto, N., & Botter, G. (2021). Time-lapse visualization of spatial and temporal patterns of stream network dynamics. *Hydrological Processes*, *35*(2). https://doi.org/10.1002/hyp.14053

Feng, X., Porporato, A., & Rodriguez-Iturbe, I. (2013). Changes in rainfall seasonality in the tropics. *Nature Climate Change*, *3*(9), 811–815. https://doi.org/10.1038/nclimate1907

Garbin, S., Celegon, E. A., Fanton, P., & Botter, G. (2019). Hydrological controls on river network connectivity. *Royal Society Open Science*, *6*(2), 181428. https://doi.org/10.1098/rsos.181428

Gupta, V. K., Waymire, E., & Wang, C. T. (1980). A representation of an instantaneous unit hydrograph from geomorphology. *Water Resources Research*, *16*(5), 855–862. https://doi.org/10.1029/WR016i005p00855

Gupta, V. K., Waymire, E. D., & Rodríguez-Iturbe, I. (1986). On scales, gravity and network structure in basin runoff. In *Scale problems in hydrology* (pp. 159–184). Springer. https://doi.org/10.1007/978-94-009-4678-1_8

Hansen, A., & Singh, A. (2018). High-frequency sensor data reveal across-scale nitrate dynamics in response to hydrology and biogeochemistry in intensively managed agricultural basins. *Journal of Geophysical Research: Biogeosciences*, *123*(7), 2168–2182. https://doi.org/10.1029/2017JG004310

Hooshyar, M., Singh, A., Wang, D., & Foufoula-Georgiou, E. (2019). Climatic controls on landscape dissection and network structure in the absence of vegetation. *Geophysical Research Letters*, *46*(6), 3216–3224. https://doi.org/10.1029/2019GL082043

Horton, R. E. (1945). Erosional development of streams and their drainage basins; hydrophysical approach to quantitative morphology. *The Geological Society of America Bulletin*, *56*(3), 275–370. https://doi.org/10.1130/0016-7606%281945%2956%5B275:edosat%5D2.0.co;2

Ingram, W. (2016). Increases all round. *Nature Climate Change*, *6*(5), 443–444. https://doi.org/10.1038/nclimate2966

Jensen, C. K., McGuire, K. J., McLaughlin, D. L., & Scott, D. T. (2019). Quantifying spatiotemporal variation in headwater stream length using flow intermittency sensors. *Environmental Monitoring and Assessment*, *191*(4), 1–19. https://doi.org/10.1007/s10661-019-7373-8

Kiffney, P. M., Greene, C. M., Hall, J. E., & Davies, J. R. (2006). Tributary streams create spatial discontinuities in habitat, biological productivity, and diversity in mainstem rivers. *Canadian Journal of Fisheries and Aquatic Sciences*, *63*(11), 2518–2530. https://doi.org/10.1139/f06-138

Kirkby, M. J. (1976). Tests of the random network model, and its application to basin hydrology. *Earth Surface Processes*, *1*(3), 197–212. https://doi.org/10.1002/esp.3290010302

Larsen, L. G., Choi, J., Nungesser, M. K., & Harvey, J. W. (2012). Directional connectivity in hydrology and ecology. *Ecological Applications*, *22*(8), 2204–2220. https://doi.org/10.1890/11-1948.1

Li, H., & Sivapalan, M. (2011). Effect of spatial heterogeneity of runoff generation mechanisms on the scaling behavior of event runoff responses in a natural river basin. *Water Resources Research*, *47*(3). https://doi.org/10.1029/2010WR009712

Mann, H. B., & Whitney, D. R. (1947). On a test of whether one of two random variables is stochastically larger than the other. *The Annals of Mathematical Statistics*, 50–60. https://doi.org/10.1214/aoms/1177730491

Marani, A., Rigon, R., & Rinaldo, A. (1991). A note on fractal channel networks. *Water Resources Research*, *27*(12), 3041–3049. https://doi.org/10.1029/91WR02077

McNamara, J. P., Ziegler, A. D., Wood, S. H., & Vogler, J. B. (2006). channel head locations with respect to geomorphologic thresholds derived from a digital elevation model: A case study in northern Thailand. *Forest Ecology and Management*, *224*(1–2), 147–156. https://doi.org/10.1016/j.foreco.2005.12.014

Mesa, O. J., & Mifflin, E. R. (1986). On the relative role of hillslope and network geometry in hydrologic response. In *Scale problems in hydrology* (pp. 1–17). Springer. https://doi.org/10.1007/978-94-009-4678-1_1

Montgomery, D. R., & Foufoula-Georgiou, E. (1993). Channel network source representation using digital elevation models. *Water Resources Research*, *29*(12), 3925–3934. https://doi.org/10.1029/93WR02463

Muneepeerakul, R., Bertuzzo, E., Rinaldo, A., & Rodriguez-Iturbe, I. (2008). Patterns of vegetation biodiversity: The roles of dispersal directionality and river network structure. *Journal of Theoretical Biology*, *252*(2), 221–229. https://doi.org/10.1016/j.jtbi.2008.02.001

Papalexiou, S. M., & Montanari, A. (2019). Global and regional increase of precipitation extremes under global warming. *Water Resources Research*, *55*(6), 4901–4914. https://doi.org/10.1029/2018WR024067

Perron, J. T., Richardson, P. W., Ferrier, K. L., & Lapôtre, M. (2012). The root of branching river networks. *Nature*, *492*(7427), 100–103. https://doi.org/10.1038/nature11672

Prancevic, J. P., & Kirchner, J. W. (2019). Topographic controls on the extension and retraction of flowing streams. *Geophysical Research Letters*, *46*(4), 2084–2092. https://doi.org/10.1029/2018GL081799

Ranjbar, S., Hooshyar, M., Singh, A., & Wang, D. (2018). Quantifying climatic controls on river network branching structure across scales. *Water Resources Research*, *54*(10), 7347–7360. https://doi.org/10.1029/2018WR022853

Rice, S. P., Ferguson, R. I., & Hoey, T. B. (2006). Tributary control of physical heterogeneity and biological diversity at river confluences. *Canadian Journal of Fisheries and Aquatic Sciences*, *63*(11), 2553–2566. https://doi.org/10.1139/f06-145

Rigon, R., Rodriguez-Iturbe, I., Maritan, A., Giacometti, A., Tarboton, D. G., & Rinaldo, A. (1996). On Hack's law. *Water Resources Research*, *32*(11), 3367–3374. https://doi.org/10.1029/96wr02397

Rodriguez-Iturbe, I., Muneepeerakul, R., Bertuzzo, E., Levin, S. A., & Rinaldo, A. (2009). River networks as ecological corridors: A complex systems perspective for integrating hydrologic, geomorphologic, and ecologic dynamics. *Water Resources Research*, *45*(1). https://doi.org/10.1029/2008WR007124

Rodriguez-Iturbe, I., & Rinaldo, A. (2001). *Fractal river basins: Chance and self-organization*. Cambridge University Press.

Rodríguez-Iturbe, I., & Valdés, J. B. (1979). The geomorphologic structure of hydrologic response. *Water Resources Research*, *15*(6), 1409–1420. https://doi.org/10.1029/WR015i006p01409

Sassolas-Serrayet, T., Cattin, R., & Ferry, M. (2018). The shape of watersheds. *Nature Communications*, *9*(1), 1–8. https://doi.org/10.1038/s41467-018-06210-4

Scheidegger, A. E. (1967). On the topology of river nets. *Water Resources Research*, *3*(1), 103–106. https://doi.org/10.1029/WR003i001p00103

Schumm, S. A. (1956). Evolution of drainage systems and slopes in badlands at Perth Amboy, New Jersey. *The Geological Society of America Bulletin*, *67*(5), 597–646. https://doi.org/10.1130/0016-7606%281956%2967%5B597:eodsas%5D2.0.co;2

Shreve, R. L. (1966). Statistical law of stream numbers. *The Journal of Geology*, *74*(1), 17–37. https://doi.org/10.1086/627137

Singh, A., Reinhardt, L., & Foufoula-Georgiou, E. (2015). Landscape reorganization under changing climatic forcing: Results from an experimental landscape. *Water Resources Research*, *51*(6), 4320–4337. https://doi.org/10.1002/2015WR017161

Stewart-Koster, B., Kennard, M. J., Harch, B. D., Sheldon, F., Arthington, A. H., & Pusey, B. J. (2007). Partitioning the variation in stream fish assemblages within a spatio-temporal hierarchy. *Marine and Freshwater Research*, *58*(7), 675–686. https://doi.org/10.1071/MF06183

Strahler, A. N. (1957). Quantitative analysis of watershed geomorphology. *Eos, Transactions American Geophysical Union*, *38*(6), 913–920. https://doi.org/10.1029/TR038i006p00913

Tarboton, D. G., Bras, R. L., & Rodriguez-Iturbe, I. (1992). A physical basis for drainage density. *Geomorphology*, *5*(1–2), 59–76. https://doi.org/10.1016/0169-555X(92)90058-V

Tejedor, A., Singh, A., Zaliapin, I., Densmore, A. L., & Foufoula-Georgiou, E. (2017). Scale-dependent erosional patterns in steady-state and transient-state landscapes. *Science Advances*, *3*(9), e1701683. https://doi.org/10.1126/sciadv.1701683

Tokunaga, E. (1978). Consideration on the composition of drainage networks and their evolution. *Geographical Reports of Tokyo Metropolitan University*, *13*, 1–27.

Troutman, B. M., & Karlinger, M. R. (1985). Unit hydrograph approximations assuming linear flow through topologically random channel networks. *Water Resources Research*, *21*(5), 743–754. https://doi.org/10.1029/WR021i005p00743

Ward, N. D., Megonigal, J. P., Bond-Lamberty, B., Bailey, V. L., Butman, D., Canuel, E. A., et al. (2020). Representing the function and sensitivity of coastal interfaces in Earth system models. *Nature Communications*, *11*(1), 1–14. https://doi.org/10.1038/s41467-020-16236-2

Wilcoxon, F. (1945). Individual comparisons by ranking methods. *Biometrics Bulletin*, *1*(6), 80–83. https://doi.org/10.2307/3001968

Willett, S. D., McCoy, S. W., Perron, J. T., Goren, L., & Chen, C. Y. (2014). Dynamic reorganization of river basins. *Science*, *343*(6175). https://doi.org/10.1126/science.1248765

Wohl, E., Brierley, G., Cadol, D., Coulthard, T. J., Covino, T., Fryirs, K. A., et al. (2019). Connectivity as an emergent property of geomorphic systems. *Earth Surface Processes and Landforms*, *44*(1), 4–26. https://doi.org/10.1002/esp.4434

Zaliapin, I., Foufoula-Georgiou, E., & Ghil, M. (2010). Transport on river networks: A dynamic tree approach. *Journal of Geophysical Research: Earth Surface*, *115*(F2). https://doi.org/10.1029/2009JF001281

Zanardo, S., Zaliapin, I., & Foufoula-Georgiou, E. (2013). Are American rivers Tokunaga self-similar? New results on fluvial network topology and its climatic dependence. *Journal of Geophysical Research: Earth Surface*, *118*(1), 166–183. https://doi.org/10.1029/2012JF002392

References From the Supporting Information

Albert, R., & Barabási, A. L. (2002). Statistical mechanics of complex networks. *Reviews of Modern Physics*, *74*(1), 47. https://doi.org/10.1103/RevModPhys.74.47

Gabrielov, A., Keilis-Borok, V., Sinai, Y., & Zaliapin, I. (2008). Statistical properties of the cluster dynamics of the systems of statistical mechanics. *ESI Lecture Notes in Mathematics and Physics: Boltzmann's Legacy*, 203–216. https://doi.org/10.4171/057-1/13

Maher, B. A. (2002). Uprooting the tree of life: A proposed theory has researchers debating life's origins--again. *The Scientist*, *16*(18), 26–28.

Witten, T. A., Jr, & Sander, L. M. (1981). Diffusion-limited aggregation, a kinetic critical phenomenon. *Physical Review Letters*, *47*(19), 1400–1403. https://doi.org/10.1103/PhysRevLett.47.1400

Zaliapin, I., Wong, H. H. L., & Gabrielov, A. (2005). Inverse cascade in a percolation model: Hierarchical description of time-dependent scaling. *Physical Review E*, *71*(6), 066118. https://doi.org/10.1103/PHYSREVE.71.066118